

# Electrical-to-Optical and Optical-to-Electrical (E/O and O/E) converter measurements

MS4640B Series Vector Network Analyzer, VectorStar  
 MS4652XB Series Vector Network Analyzer, ShockLine  
 MS46322B Series Vector Network Analyzer, ShockLine  
 MS46122B Series Vector Network Analyzer, ShockLine

As fiber and free-space optical communication bandwidths increase, the need for very high speed optical modulators and detectors has also increased. The frequency response characterization of these electrical-to-optical (E/O, modulators sometimes integrated with lasers) and optical-to-electrical (O/E, photo detectors and receivers) converters can be important in terms of such parameters as bandwidth, flatness, phase linearity and group delay. The Anritsu MS464XX VectorStar™ and ShockLine™ VNAs have a number of measurement utilities to facilitate this kind of analysis and, coupled with the MN4765B O/E calibration module (for 850, 1060, 1310 and 1550 nm measurements with up to 40 GHz (for 850 and 1060 nm), 70 GHz (for 1310 or 1550 nm) or 110 GHz (1550 nm) of bandwidth) or some other calibration device, some level of measurement traceability is possible. This application note will discuss some of the measurements of interest, setup considerations, possible measurement performance, and examples of measurement procedures.

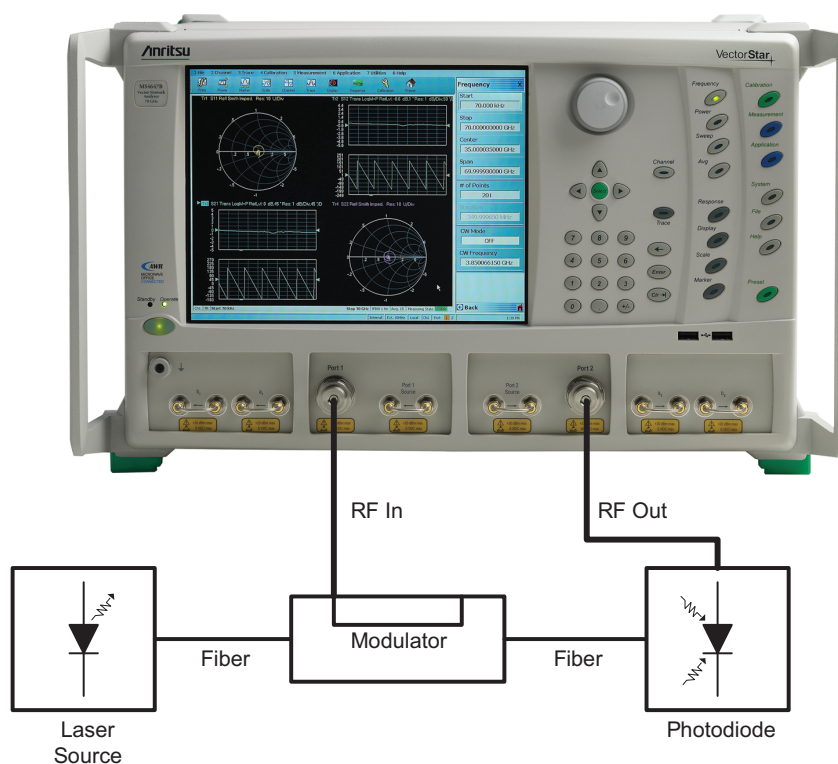


Figure 1: A general 2-port E/O or O/E measurement setup is shown here. In some cases, the laser and modulator may be one assembly. The photodiode may be integrated with amplifiers or other components into a photoreceiver.\*

\* The connections to the VNA test ports are the same for ShockLine Vector Network Analyzers.

## Introduction and background

Conceptually, the job of the optical modulator is to place a microwave signal as modulation onto an optical carrier. Similarly, the job of the photodetector or receiver is to recover that modulation and regenerate the microwave signal. For a VNA-based measurement, both directions of conversion are required so that the processing can occur in the microwave or modulation signal domain. The result is a setup like that shown in Figure 1. The optical carrier is generated (usually) by a coherent laser source (which may be integrated with the modulator), modulation is applied, and then the modulation is recovered. Optical fiber is shown as the media in Figure 1 but it could be some other optical guiding medium or free-space in some cases. The VNA acts as a microwave stimulus (port 1 in the figure) and receiver (port 2 in the figure). Three and four port cases are also possible, involving multiple converters or differential ones, which will be discussed later in this application note.

Since the measurement results will be classed as normal S-parameters, one may wonder how these relate to the actual optical behavior of the components. In some sense, they all become relative because the conversion between domains introduces dependencies on optical laser power, optical path losses (usually small) and other absolute shifts. Thus, the real measure of conversion is essentially a responsivity slope between the optical and electrical domains as illustrated in Figure 2. The S-parameters that appear on the instrument display for an O/E or an E/O component then represent a relative responsivity measure (in both magnitude and phase). Often, the frequency response of this quantity is of interest as that determines bandwidth; and magnitude vs. frequency plot gives this information. The phase linearity and group delay are both ways of looking at the deviation from a purely linear phase function that can be an important assessment of potential phase-related modulation distortion. Return loss of the component may also be of interest but that is a purely microwave measurement.

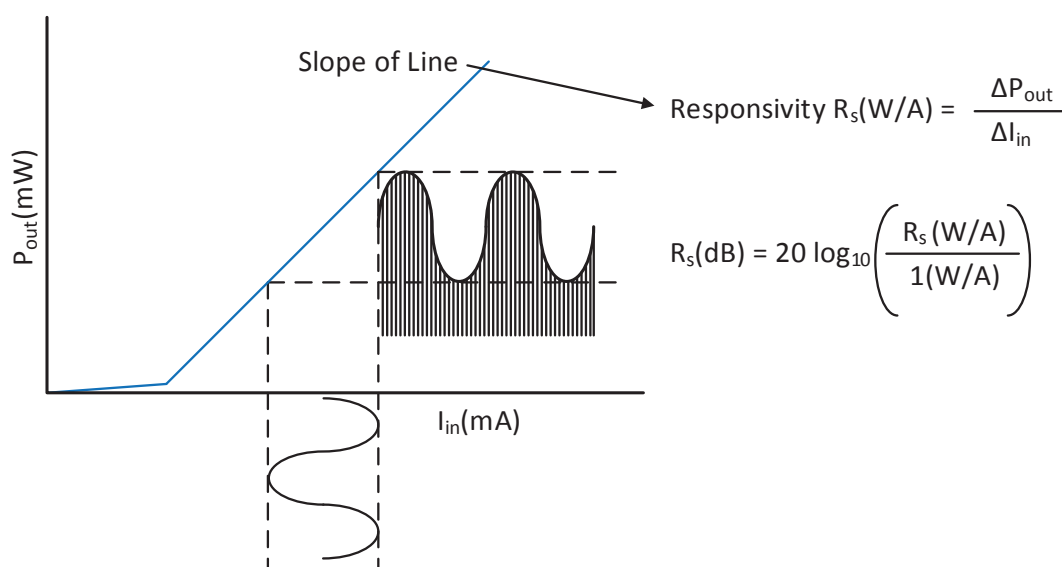


Figure 2: The concept of responsivity is shown here. The conversion parameters of the O/E and E/O devices measured with the VNA are essentially measures of responsivity.

The next question may be how the measurements are conducted. The starting point is a two-port VNA calibration. This calibration establishes reference planes at the microwave ports of the optical devices as shown in Figure 3 (often coaxial ports; but could be waveguide, in a fixture, on-wafer, etc...). The next step is the use of an O/E calibration device such as the MN4765B, which is a wide bandwidth photodetector housed in a thermally controlled module with carefully designed bias circuitry. This module is characterized at a traceable facility using electro-optic sampling techniques (or references derived from that) so its frequency response (in magnitude and phase) is well-known with established uncertainties<sup>1,2</sup>. If such a calibration device is the detector in Figure 1, then its effects can be de-embedded<sup>3</sup> since those behaviors are known. This then moves the reference plane to the optical side of the photodiode/calibration detector as shown in Figure 3. Now a measurement of S21 will describe the loss and phase of the modulator alone (plus some effect of the fiber which will be discussed). This frequency response (magnitude and phase) gives the required performance information discussed earlier when combined with the microwave reflection measurement (S11) of the modulator RF port that comes for 'free' with the calibrated VNA measurement.

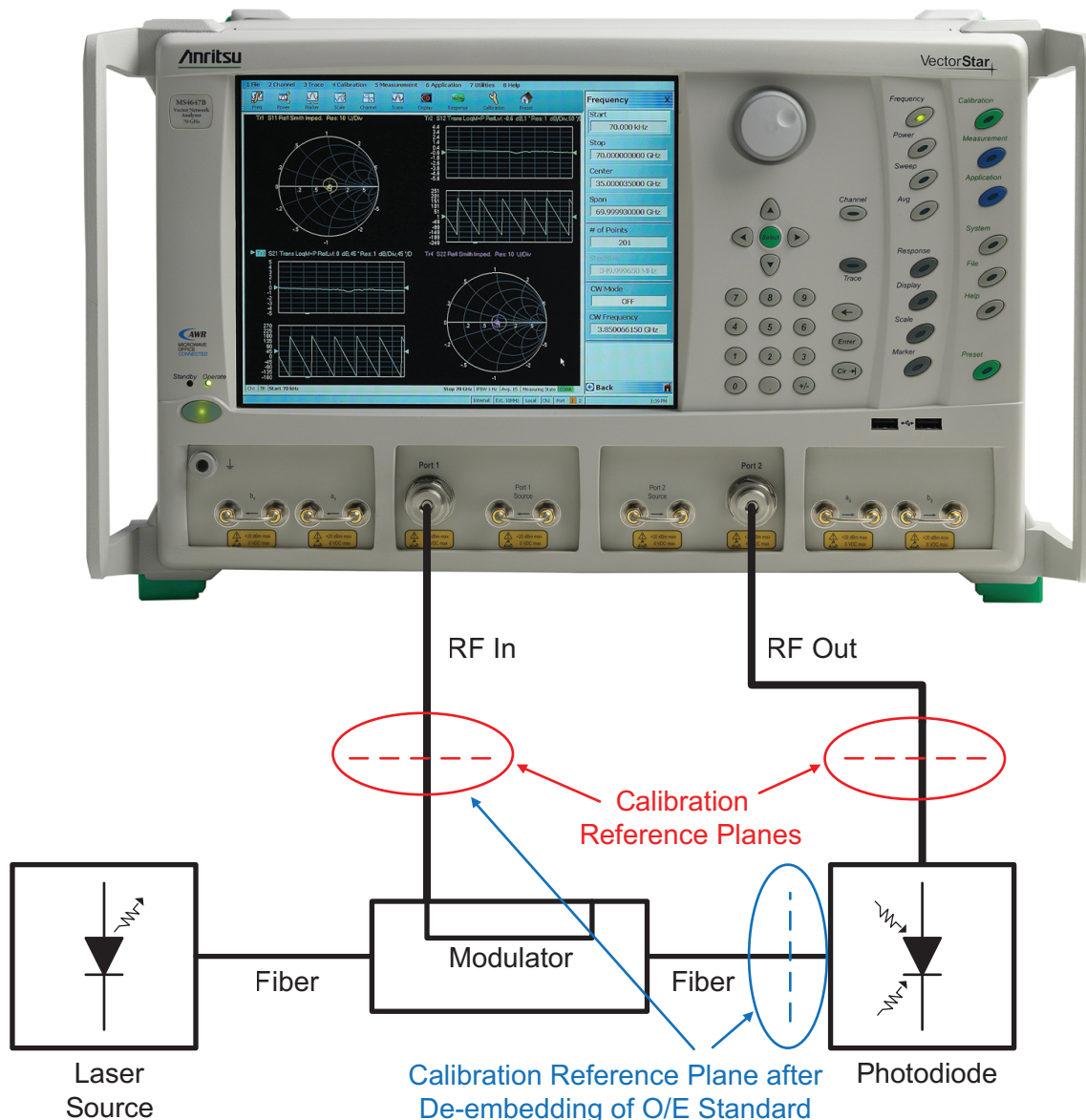


Figure 3: Reference plane placement is shown here. A calibration is done in coax, waveguide, or some other electrical media and the de-embedding function, via the O/E-E/O measurement utility, of the VNA are used together with optical data to move a reference plane into the optical domain.

<sup>1</sup> D. F. Williams, P. D. Hale, T. S. Clement, and J. M. Morgan, "Calibrating electro-optic sampling systems," 2001 Int. Micr. Symp. Dig., pp. 1527-1530, May 2001.

<sup>2</sup> P. D. Hale and C. M. Wang, "Calibration service for evaluating and expressing optoelectronic frequency response at 1319nm for combined photodiode/RF power sensor transfer standards," NIST Special Publ. 250-51, 1999.

<sup>3</sup> See the embedding/de-embedding sections of chapter 10 in the "VectorStar Measurement Guide," Anritsu Document #10410-00318 for more detailed information about embedding/de-embedding. As will be seen, the de-embedding process can be additionally automated for O/E and E/O measurements.

An example plot of the conversion response of a 50 GHz photodetector, operating at 1550 nm, is shown in Figure 4. From the magnitude response, the 3-dB bandwidth is indeed around 50 GHz but the roll-off is sufficiently slow, so this device is commonly used beyond 65 GHz. The phase response is also shown in the figure but the linear portion has not been removed. The group delay plot (derivative of phase with respect to frequency) is often a more convenient way of looking at the phase behavior. Towards 50 GHz, there are some deviations from flat group delay (equivalent to deviations from linear phase) that are not surprising in view of the device's bandwidth. If being used as a characterization device, these deviations are not important since they can be well-characterized (to beyond 65 GHz in this case). In terms of using the device in actual applications, the group delay and amplitude effects at higher frequencies would have to be considered.

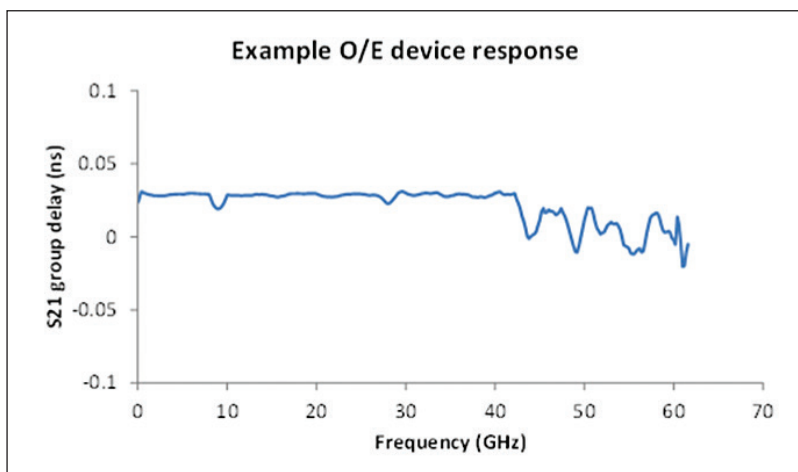
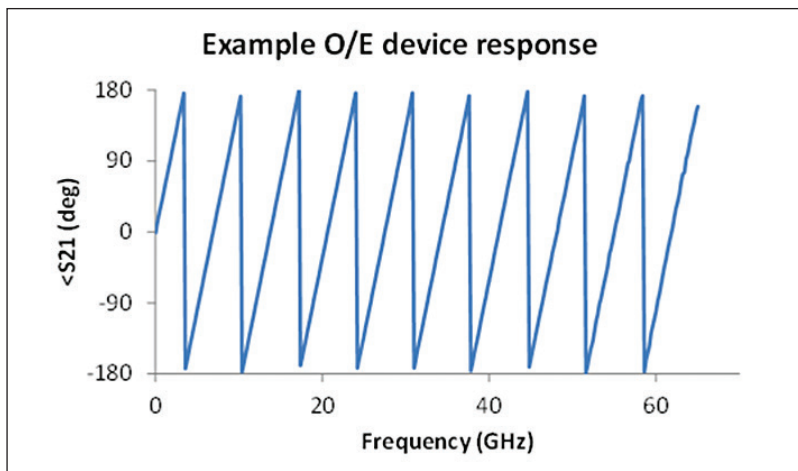
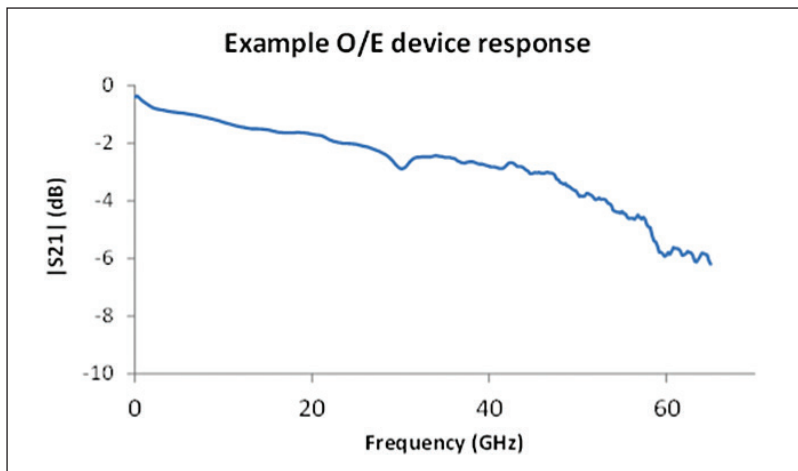


Figure 4: The characteristics of an example O/E device are shown here.

If one now wanted to measure a different O/E device (not a calibration module); one could then insert that detector into the setup of Figure 3 and instead, now de-embed the modulator response that was just measured previously. In this case, because it is a second level de-embed, there may be some elevation of uncertainties that will be discussed. One could also obtain an E/O calibration device and use that instead, in a one-step process.

The de-embedding (or sequential de-embedding) steps form the basis of this O/E-E/O measurement utility. The key points are controlling traceability and uncertainties throughout the process when multiple devices are being used to control match so minimal additional artifacts are introduced, and to not try to de-embed what cannot be de-embedded. This last point is important in that inner-plane (optical) match is not known and the transmission path is unilateral anyway so there are no multiple reflections within the DUT assembly to remove.

All of these measurement aids are available under the O/E-E/O button on the Measurements menu. As might have been guessed from the previous discussion, these approaches naturally separate based on whether the target is an O/E device (detector, receiver...) or an E/O device (modulator...). The menu selections, as shown in Figure 5, delineate that choice.

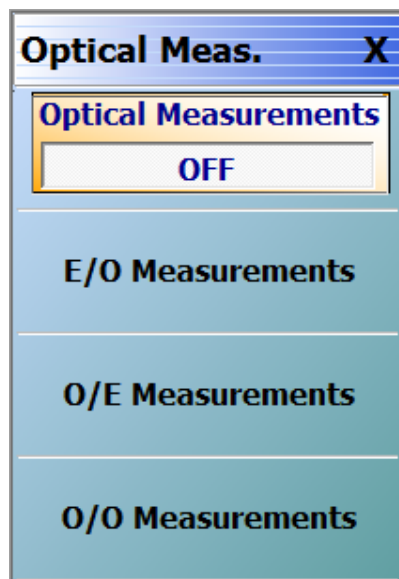


Figure 5: Under the Measurements/(O/E-E/O) menu are the two selections based on which type of device is to be solved for.

O/O measurements are also possible where both converters are de-embedded from the measurement leaving an RF characterization of the optical path between them. This can be used for analyzing the instantaneous bandwidth capabilities of optical attenuators, amplifiers, and other signal processing components. Note that there is no match correction in the optical domain.

## Measurement setups and considerations

It is not the intent of this application note to fully cover the optical setup details but some common issues and concerns will be discussed. More general information of fiber optic measurement setups can be found elsewhere<sup>4,5</sup>.

### Optical linearity

The linearity of the characterized photodiode directly affects the accuracy of the measurement and the optical input power at which RF photocurrent will remain linear is important. One way to check that the measurement path is still linear is to normalize the S21 plot against itself and increase the optical power to see if there is a gross sensitivity. For example, set the optical laser power to 4 or 0 dBm with the setup like that of Figure 1. Store the resulting S21 to memory (under the Display/View Trace menu) and then view DataMemMath (data divided by memory). Now increase the laser power in 1 dB steps until some compression is seen in the normalized plot on the scale of 2 dB/div. At that point, decrease the optical power level until it is out of compression. Make sure that the maximum DC current for the photodiode is not exceeded.

### Laser power and photodetector bias sequencing

Always make sure the photodiode is biased properly before turning the laser on. Improper bias or no bias can degrade photodiode performance and can also result in damage. Instructions on handling and biasing of the photodiode are shipped with the characterized photodiode accessory. Always observe ESD precautions as these devices are very sensitive to static discharge.

### Optical fiber lengths

The measurement setup will typically require optical fibers to interconnect optical components with different connectors. For example, a modulator with an FC/PC connector at the output will require an optical patch cord to adapt to the FC/APC connector on the input of the characterized photodiode accessory. Optical fibers have negligible frequency dependent loss over microwave modulation bandwidths. Thus, adding short lengths of optical patch cords to the setup does not affect the accuracy of transfer function measurements. To avoid certain polarization-related issues, it is recommended to keep the patch cord length under 10 meters. Using a fiber appropriate for the wavelength involved can help minimize measurement stability issues.

### Modulator bias control

Lithium niobate modulators are generally biased using a modulator bias controller (MBC) to control the operating point of the modulator. When biased in quadrature, the input RF signal linearly modulates the optical carrier. Note that when an MBC is applied, it must be designed for small signal operation. The default power from the Port 1 test port is -10 dBm for the MS4647B when equipped with options 051, 061 or 062. This level results in a modulation depth of <10% for most commercially available modulators. If a different model VNA or a different option configuration is being used, it may be required to drop the VNA power level from the default setting to ensure that the modulator is operating linearly. Different technology modulators may have different linearity limits so it may be required to consult the manufacturer of that device.

A DC power supply can be used in place of an MBC. However, the stability of the measurement may be degraded due to drift in the modulator's bias point.

### Connector care

It is important to establish proper cleaning procedures when connecting fiber optic devices together. Fiber optic cores are made of glass and can easily be scratched or chipped if care is not taken. The connectors found on the MN4765B are of the FC/APC type. APC (Angled Physical Contact) is chosen to help minimize back-reflection. The 8° angle at the end-face of the APC connector has an optical return loss of better than 50 dB. DFB lasers require large amounts of reflection isolation to function properly. The optical return loss from a common PC connector can be 30 dB or worse, depending upon the polish and cleanliness of the connector.

---

<sup>4</sup> D. Derickson, Fiber optic test and measurement, Prentice-Hall, pp. 252-263 and 621-638, 1998.

<sup>5</sup> J. Hecht, Understanding fiber optics, Prentice-Hall, pp. 28-31, 1999.

The following are some tips to help ensure quality connections.

- Always clean optical connectors after every connection.
- Use a fiber optic scope often to ensure there are no defects on the connector end face that can cause damage to other connectors.
- Use insertable patch cords for expensive devices that require many connections.
- Always use a cloth that is free of fiberglass to clean the connectors. If necessary, use alcohol to remove stubborn dirt and oil. Thoroughly remove any alcohol residue before reconnecting.
- Avoid using any oils for connecting two cables together. Oils are messy and very difficult to clean up.
- Optical connectors do not need torque. Some connections are better when the two fibers are barely touching. Tightening the connector too much will result in higher insertion loss, more reflection, and in some cases damage to the connector.
- Always observe proper mating to APC connectors. Connecting APC to PC connectors will damage the connectors.

### Example 2-port procedures

With the physical setup described, the next task is to use the measurement utilities inside the VectorStar VNA. Consider first the case of a 2-port E/O measurement where one has a characterized O/E device (such as the MN4765B). The dialog for this measurement is shown in Figure 6 (the system automatically detects if it is a 4-port configuration in which case one of the later dialogs would be displayed instead). One choice that has to be made is the port configuration. The default is to have the E/O device connected to port 1 of the VNA, but this can be changed.

The other major requirement is a 2-port VNA calibration. This dialog assumes that the calibration has already been done with the desired method, frequency range, etc. and saved (using Save Setup under the file menu) as a .chx file. Most of the setup parameters are obvious:

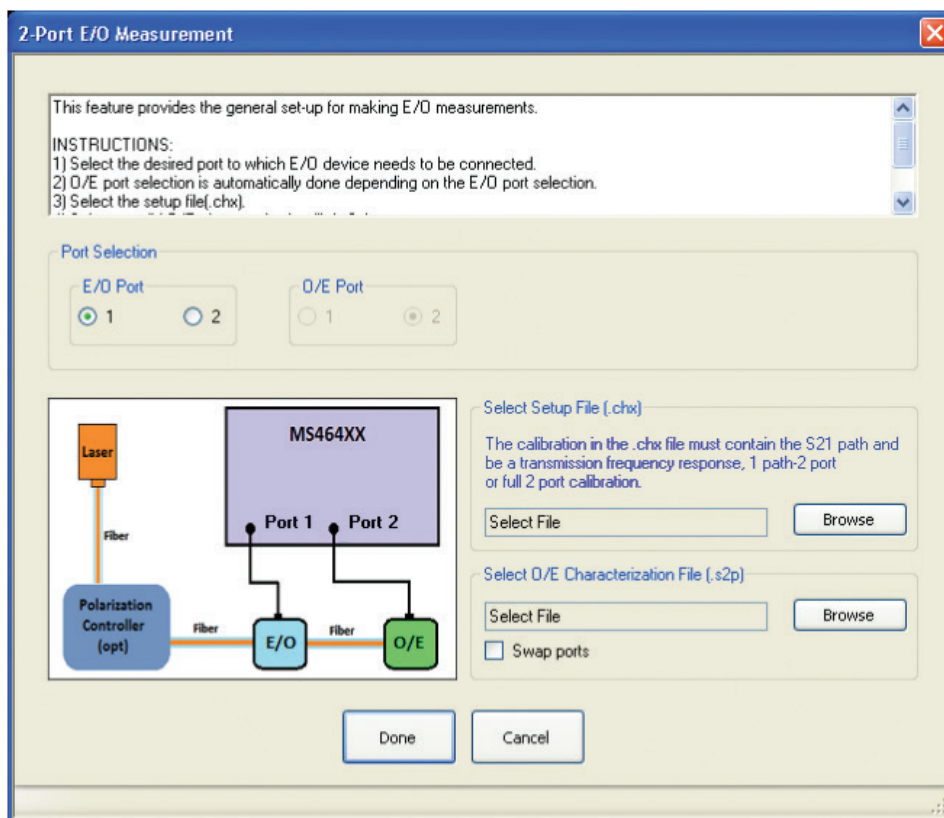


Figure 6: The dialog for 2-port E/O measurements is shown here.

- Frequency range and number of points (dictated by the bandwidth of the DUT among other test requirements)
- Power level (this depends on the linear drive range of the modulator as discussed above and the maximum available power of the VNA, which varies with options. Generally, the higher the better within those limits for best signal-to-noise ratio)
- IF Bandwidth and averaging (trade-off between measurement time and trace noise. Generally 10-100 Hz IFBW is recommended for very wideband devices since the conversion losses tend to be high and the signal-to-noise ratio is stressed). Averaging can be added for additional trace noise reduction but there is a point of diminishing returns beyond about 10 sweep-by-sweep averages or if IFBW/(pt-by-pt averages) falls below 1 Hz.
- Calibration method. The only requirement is that the calibration contain a transmission path that match the E/O->O/E path (anything beyond that is acceptable). Some of the choices:

E/O port = 1

Forward transmission tracking (1->2)

1 path – 2 port forward (1->2)

Full 2 port calibration

E/O port = 2

Reverse transmission tracking (2->1)

1 path – 2 port reverse (2->1)

Full 2 port calibration

Any calibration algorithm can be used (SOLT, SOLR, LRL, LRM...) as appropriate.

Assuming this setup file is now available, it can be loaded in the dialog of Figure 6 as can the O/E characterization file (in a .s2p file format). Note the 'swap ports' checkbox availability near the characterization portion of the dialog box. It is always assumed that the dominant path in the characterization file is the S21 parameter. If the file was constructed differently (e.g., S12 was the measurement path for the calibration device), then selecting the checkbox will force the instrument to reorder the ports in the file before processing.

When 'Done' is hit on this dialog, the de-embedding is applied and the resultant calibration left on the system includes the shifted reference plane as suggested by Figure 3. This state can be saved as a new setup file (again using the Save Setup command under the File menu) if desired. Note that to go back to the non-de-embedded state, one can recall the old setup file that was just loaded in the dialog box. At this point, one can make measurements of any number of E/O devices and save the results using any of the usual techniques.

The O/E measurement setup is quite similar and that dialog is shown in Figure 7. The difference, of course, is that an E/O characterization file must now exist. One can generate it using the previous procedure and saving the measurement result as a .s2p file or one may already have a characterization file for the E/O device. If this is not the case, a shortcut is provided to help generate an E/O characterization file with less work. This path is triggered with the 'Go Measure E/O' button which will bring up the sub-dialog of Figure 8.

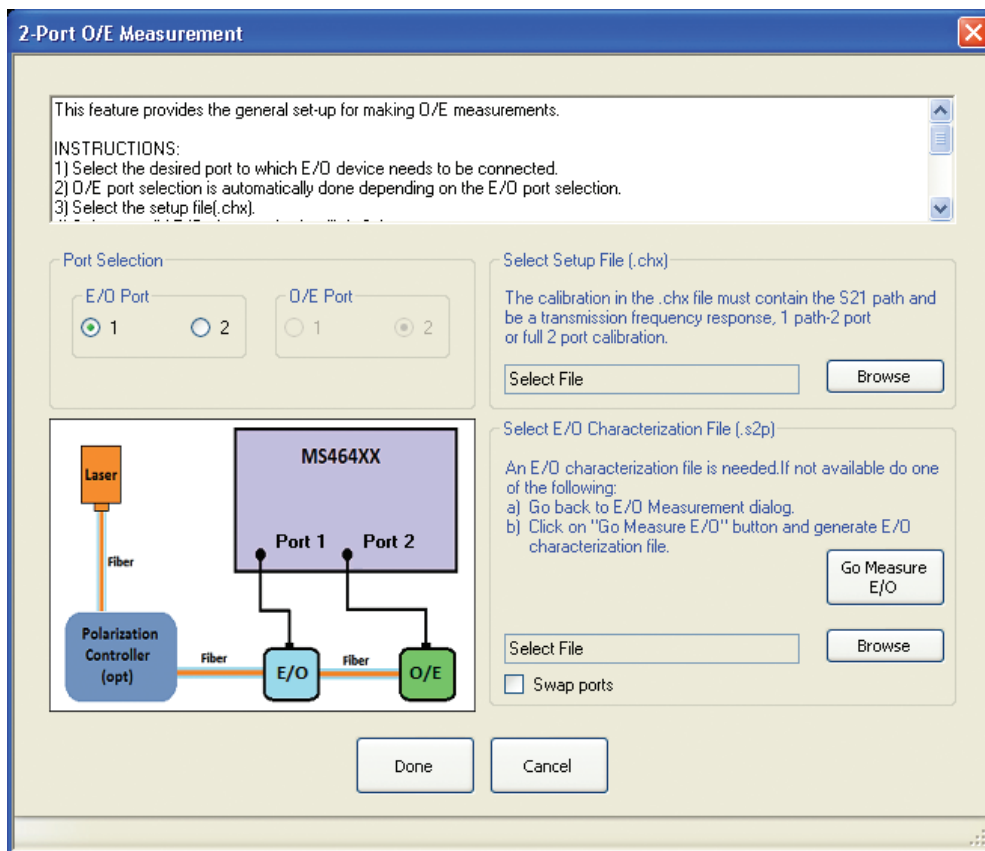


Figure 7: The dialog for 2-port O/E measurements is shown here.

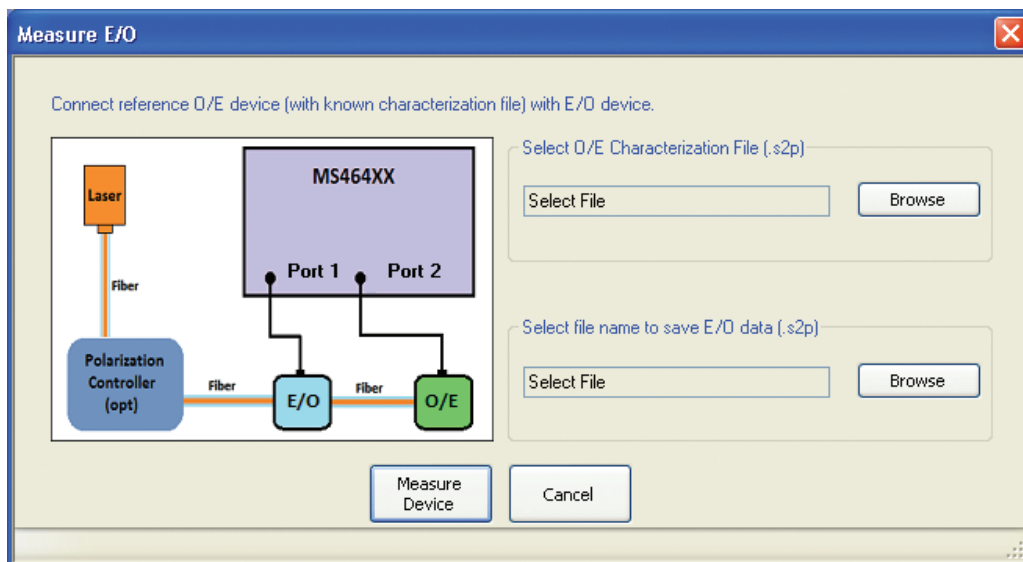


Figure 8: When measuring O/E devices, the characteristics of the E/O device must be known. If a file does not already exist, this dialog can help in doing the intermediate measurement with the help of a calibration O/E device such as the MN4765B.

Assuming one has an O/E calibration device (such as the MN4765B), this Go Measure feature allows one to load that photodetector characterization file and use the setup file found on the main O/E dialog to do a quick measurement of the modulator (or assembly). The sub-dialog also has a field to save this new E/O characterization file. When completed, one can go back to the previous dialog and hit 'Done'. The resultant setup will now have the port 1 reference plane moved to after the modulator so one can now measure any number of new O/E devices. Again, the final setup (with shifted reference planes) can be saved as can any new measurement data of the O/E devices.

A limited variety of O/O measurements can also be made where both the modulator and detector responses have been de-embedded. Optical match is in no way corrected and the fiber (including patch cords) used in the measurement will not be corrected (but normally have no notable frequency response anyway).

The dialog is very similar to that shown for E/O and O/E measurements. One must now either provide two .s2p files (one for the modulator and one for the detector-usually the MN4765X) or measure one on-the-fly (much like how the modulator was characterized for the O/E measurement process). In some sense, this on-the-fly characterization is like an O/O normalization calibration step. In any event, at the conclusion of the process, the reference planes are both in the optical domain and an O/O annunciator will be displayed.

As an example, consider the following setup:

- 2-60 GHz, 10 Hz IFBW, power -10 dBm, no averaging
- A full two-port SOLT calibration is performed using a 3654D calibration kit.
- The resulting setup file is saved as setup.chx. This setup file will include all of the above parameters including the calibration data.
- The optical assembly is hooked up with the modulator-under-test connected to port 1 and an MN4765B O/E calibration module connected to port 2 of the VNA. The laser is powered up after setting up bias control on the modulator and applying bias to the MN4765B (and, of course, connecting the fiber).
- The E/O measurement utility is invoked using the default port assignment, loading the .chx setup file and loading the characterization file of the MN4765B. Upon hitting 'Done' on the dialog, the resulting S21 measurement reflects the conversion behavior of the modulator and is shown in Figure 9. In this case, there is about 10 dB of roll-off over the bandwidth of the measurement.

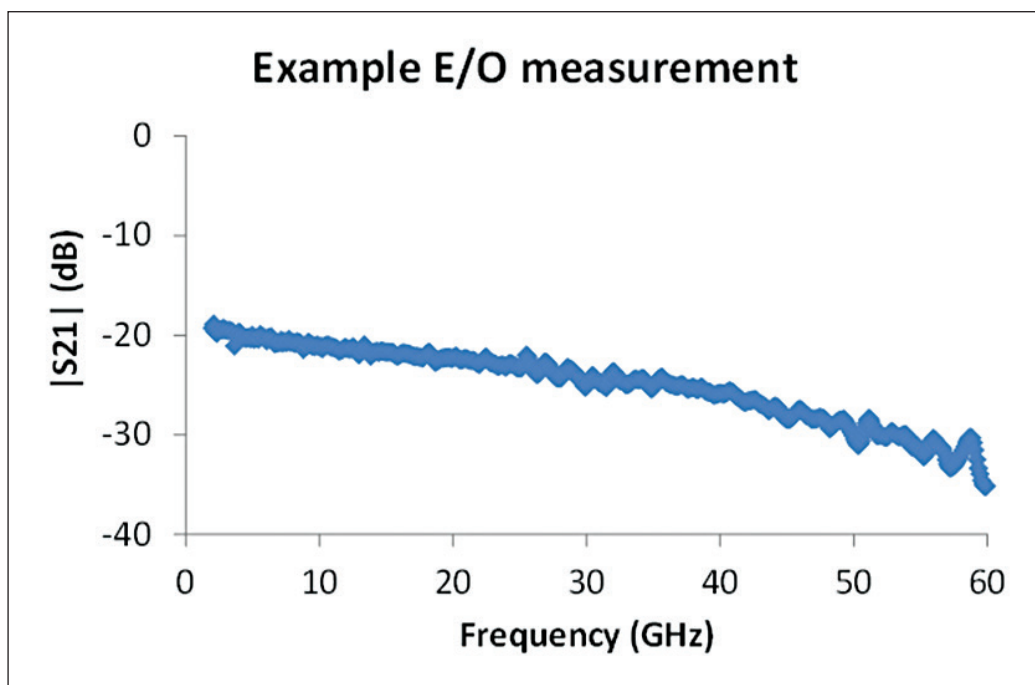


Figure 9: The results of an example 2-port E/O measurement are shown here using the procedure discussed in the text

## Example 4-port procedures and variations

When a four port VNA is used, there are obviously more port permutations possible for connections but also differential or multiport O/E and E/O devices can be handled. The measurement processes are essentially the same as for the two port cases just discussed but there are some additional logistics to handle.

### Case 1: single-ended E/O- single-ended O/E

For the case of solving for single-ended E/O device when used with a single-ended O/E device, the dialog of Figure 10 applies and the main choice is which ports are to be used. The same rules discussed in the previous section apply on the type of calibration used (in the .chx file to be loaded) except that the path selected (using the port checkboxes) must be covered by that calibration. In addition, full 3-port and 4-port calibrations can be used if desired (where the 3-port calibration must cover the ports being used). The O/E characterization file in this case is again a .s2p format file with S21 as the parameter of interest.

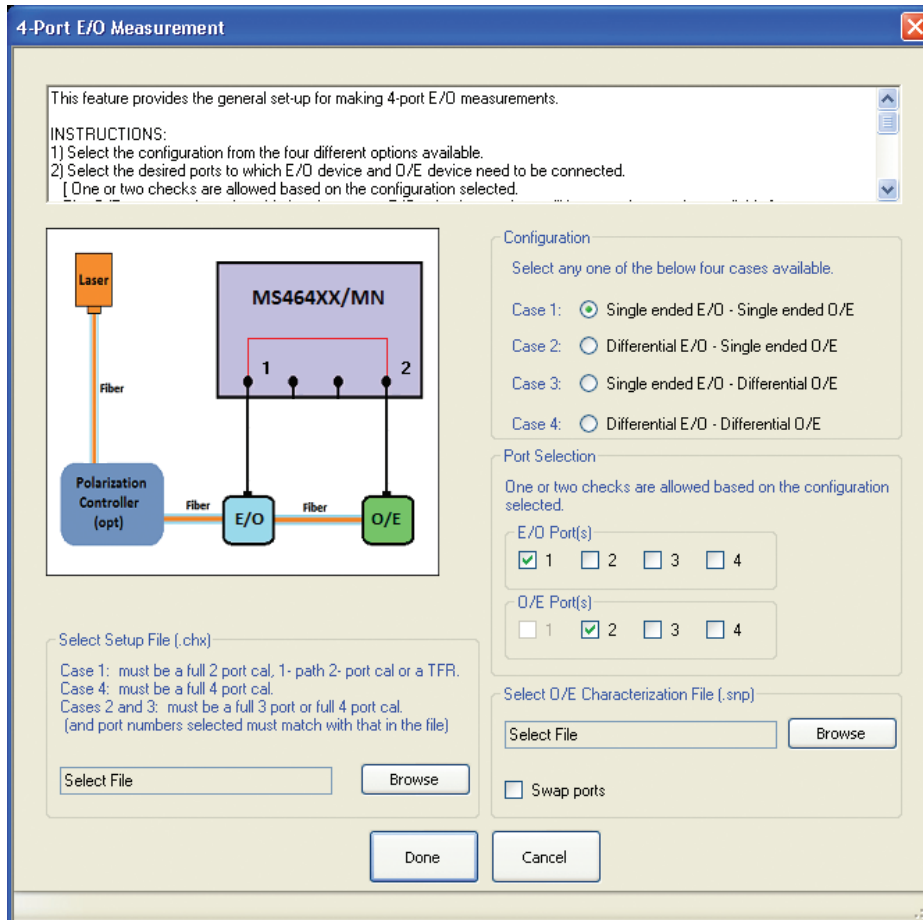


Figure 10: The dialog for 4-port E/O measurements is shown here.

For the case of one or more differential (or multiport) optical devices, the additional 'cases' apply and the dialog changes slightly as shown in Figure 11.

A few things change in these other cases:

### Case 2: differential E/O- single-ended O/E

The .chx file must contain a full 3-port calibration (using the ports in question) or a full 4-port calibration of any algorithm (including hybrids)

The O/E characterization file is still of the .s2p form (S21 is the dominant parameter)

### Case 3: single-ended E/O- differential O/E

The .chx file must contain a full 3-port calibration (using the ports in question) or a full 4-port calibration of any algorithm (including hybrids)

The O/E characterization file is of a .s3p form (S21 and S23 are dominant) or a .s4p form (S21 and S43 are dominant)

A 'reassign ports' option is now available for assigning the ports in the characterization file to match the path expectations. The current state of port reassignment is shown as a read-only field in the dialog. The default is no reassignment (1->1, 2->2, 3->3, 4->4).

### Case 4: differential E/O- differential O/E

The .chx file must contain a full 4-port calibration of any algorithm (including hybrids)

The O/E characterization file is of a .s3p form (S21 and S23 are dominant) or a .s4p form (S21 and S43 are dominant)

A 'reassign ports' option is now available for assigning the ports in the characterization file to match the path expectations.

In this case, there is also potential confusion as to how the DUT is exactly connected if it is '2 paths in parallel' instead of a true differential device pair. It is always assumed that the lower numbered E/O port is connected to the lower numbered O/E port. If two DUTs are being measured in parallel, make sure the port connections match this assumption.

As in the two port case, when one hits 'Done' to leave this dialog, the resident calibration will now have the O/E device de-embedded and the live measurements will reflect the behavior of the E/O device. Data and setups can be saved from this state as usual.

**IMPORTANT:** The .s3p and .s4p files loaded as characterization files have assumed transmission paths as detailed in the text. Use the 'Reassign ports' feature to make your file match those assumed paths.

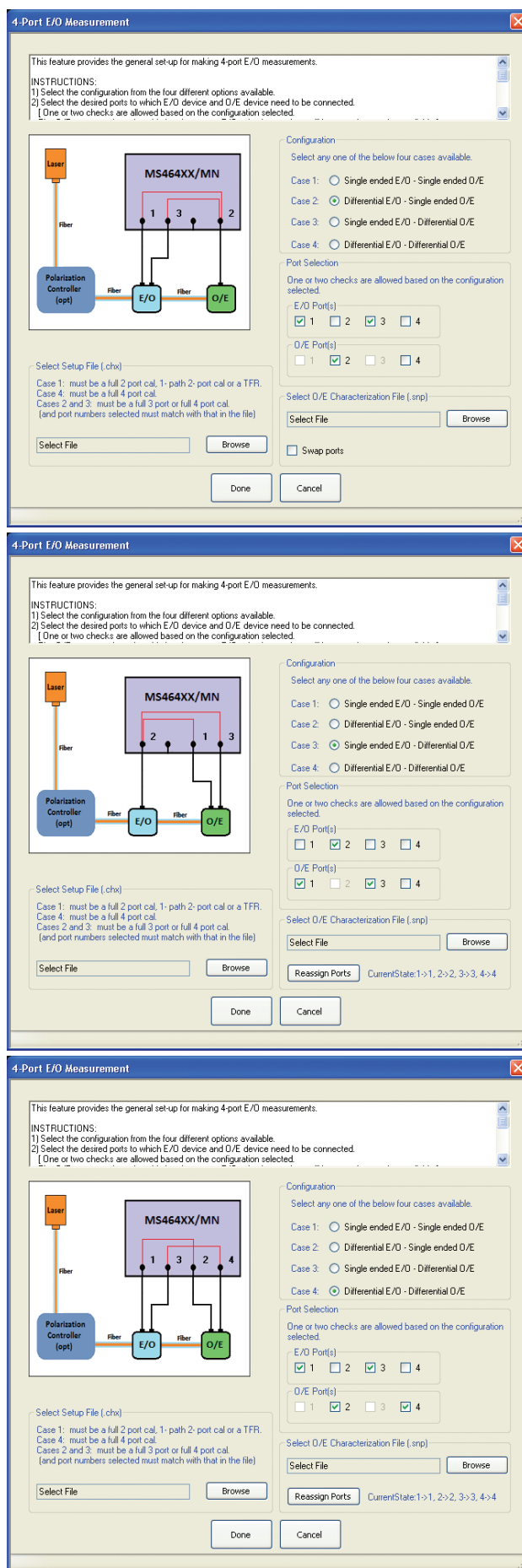


Figure 11: Variations for different DUT port structures are shown here.

## O/E Measurement Case

For the O/E measurement case, the permutations are essentially the same and these are shown in Figure 12. The only real difference is that cases 2 and 3 swap roles in terms of file types required as is obvious in the figure.

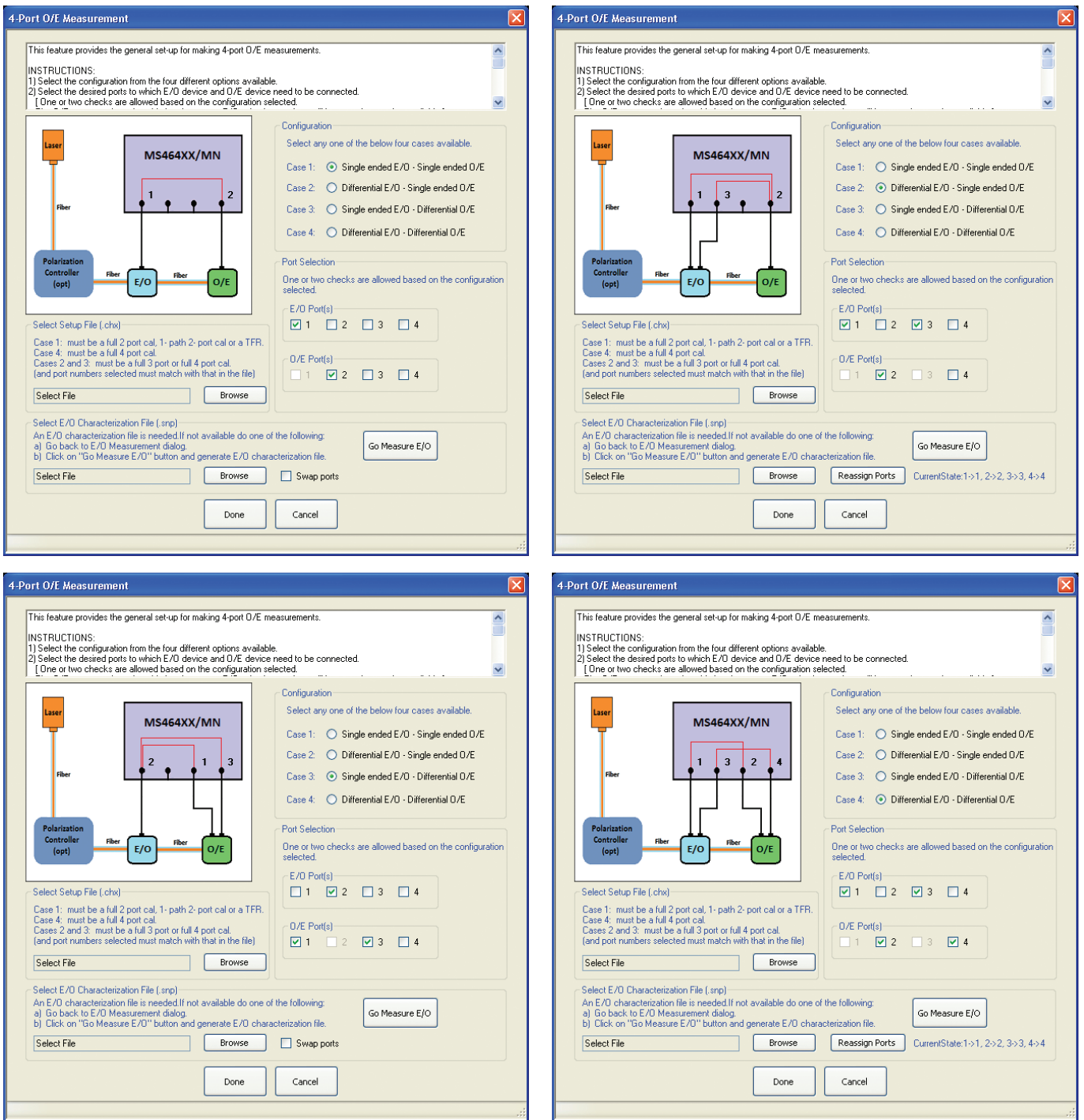


Figure 12: The dialogs for 4-port O/E measurements are shown here.

As with the two port O/E measurement case, there is a shortcut to go measure the E/O device to get its characterization file (assuming one has a characterized O/E device to start with such as the MN4765B). This shortcut sub-dialog is shown in Figure 13 and it must use the same case and port assignment as the parent dialog. In addition, the E/O file that is generated from this sub-dialog will follow the dominant port assignment paths that have been detailed in this section.

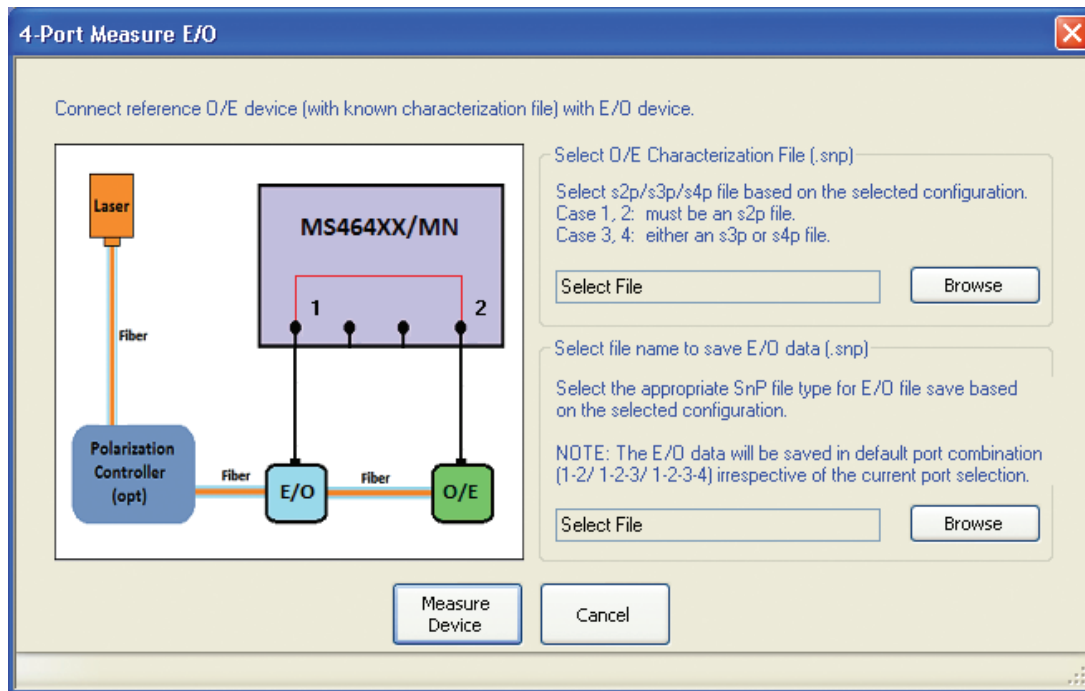


Figure 13: The 4-port intermediate measurement dialog is shown here for O/E measurements when the E/O characterization file does not already exist.

The four-port O/O measurements proceed analogously. Either .s2p files must exist for both detector (usually the MN4765B) and the modulator on a path or one of those files can be generated on-the-fly using the 'thru' optical equivalent.

As an example, consider the following setup:

- 100 MHz-65 GHz, 1000 Hz IFBW, -17 dBm drive power
- A double-path E/O device feeding a single-ended MN4765B (so this becomes case 2 under E/O measurements). The E/O device will be connected to ports 1 and 2 while the O/E device will be connected to port 3. The measurements of interest are then S31 and S32. The O/E characterization file is still of the .s2p format where S21 is the controlling parameter.
- A full three port calibration is performed using the 3654D calibration kit (SOLT) and the setup file is saved (.chx).
- The optical components are connected and powered in the appropriate order as discussed previously.
- The E/O dialog is configured as described above and, after 'Done' is selected, the resulting measurements are those of the E/O device. Some example possible measurements are shown in Figure 14. In this case, the device is not as symmetric as hoped (note the differences between S31 and S32) in terms of both conversion magnitude and group delay. A strong resonance is observed in both paths near 62 GHz and lower-Q resonances are seen in the S31 path at lower frequencies. This type of data could be useful in device optimization/redesign.

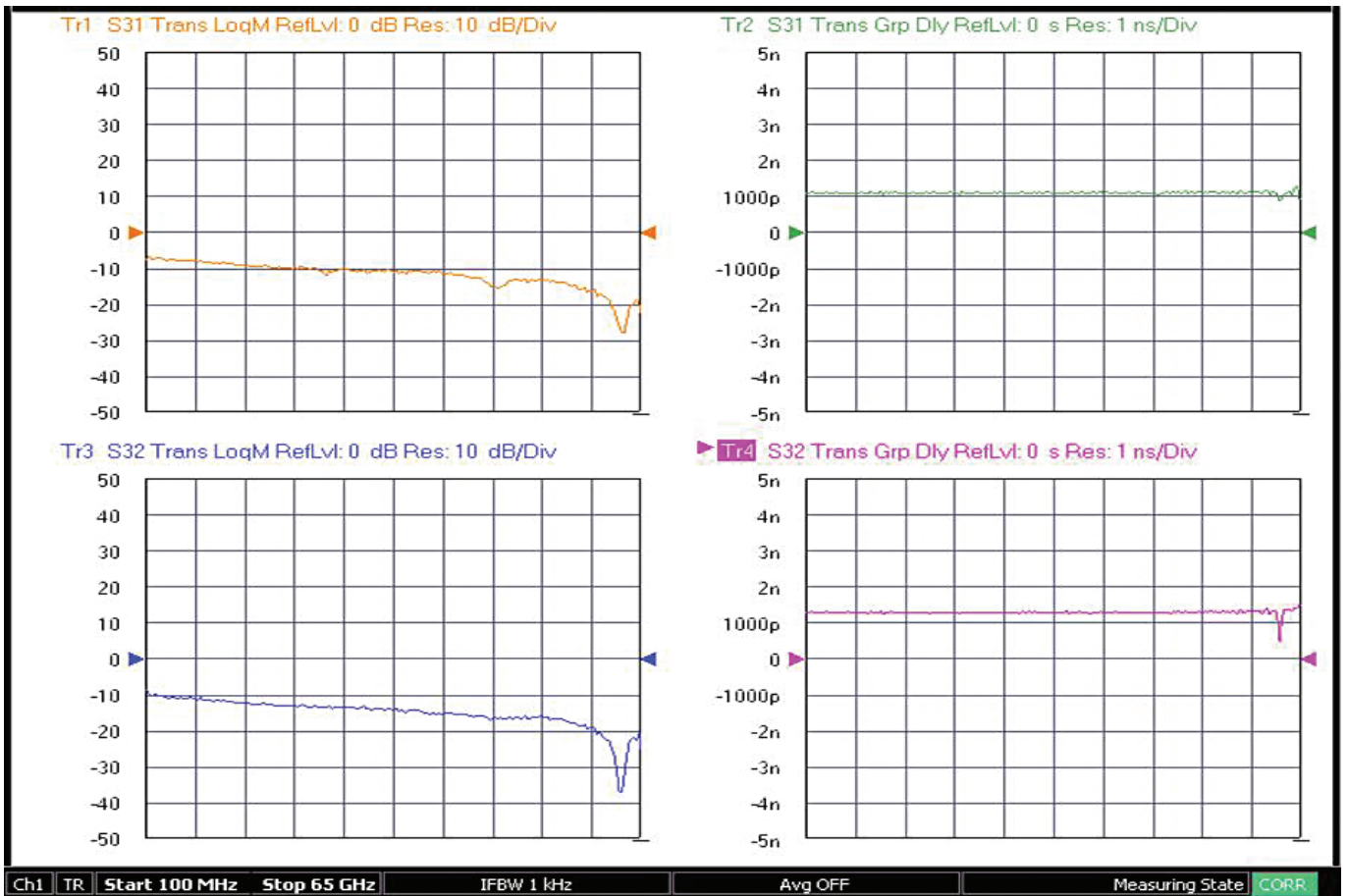


Figure 14: An example of what could be a common 'case 2' measurement is shown here. In this case, the data represents a dual-path E/O device being analyzed.

## Uncertainties

In the measurements just described, the uncertainty can be broken into two broad categories:

1. Uncertainty associated with the characterization of the calibration device (such as the MN4765B)
2. Uncertainty in the measurement with the DUT

Typically the user will purchase a characterized photodiode and receive a data file describing that device's transfer function. There is some uncertainty associated with that data based on the characterization technique.

There are different levels of characterization possible. A direct characterization using such optical techniques as electro-optic sampling<sup>6</sup> or the heterodyne method<sup>7</sup> would be termed 1<sup>st</sup> tier. It is outside the scope of this note to go into detail on these characterization techniques but they are discussed in the references and in other literature. These 1<sup>st</sup> tier characterizations are typically performed at National Metrology Institutes (NMIs, such as NIST or NPL) or large private laboratories.

A 2<sup>nd</sup> tier standard is characterized by a laboratory based on a 1<sup>st</sup> tier standard. It would be generated using a process similar to the techniques discussed here but under carefully controlled conditions (bias, temperature, wavelength, etc.) using a 1<sup>st</sup> tier standard as the characterization device. This 2<sup>nd</sup> tier device is much more commonly available (the MN4765B is an example) and the uncertainties for a 2<sup>nd</sup> tier standard will be used in later calculations. The uncertainty penalty in going to 2<sup>nd</sup> tier device is typically small (on the order of 0.1 dB additional).

When measuring the DUT, there is an uncertainty associated just with the VNA measurement which is discussed elsewhere<sup>8</sup>. Since the characterized photodiode response is then de-embedded, the characterization uncertainty must be combined with the VNA measurement uncertainty to obtain an overall value. In the case of an O/E measurement, there are actually two user measurements involved (one with a modulator and the characterized photodiode and one with that modulator and the DUT) so an additional uncertainty must also be included (note the distinction between this second level de-embed and a 2<sup>nd</sup> tier calibration device). Typically these uncertainties are all added on a root-sum-square basis since the measurements are assumed to be dominated by uncorrelated quantities.

Before proceeding to some uncertainty values, it may be useful to examine dependencies. On the VNA side, S21 uncertainty is typically quite low for medium power levels but will deviate at high signal levels (receiver compression, not an issue in these measurements) and at low signal levels (effects of the receiver noise floor). Thus the overall uncertainty will be a function of detector output signal level (getting worse as the signal level gets closer to the noise floor). Results can be improved by using higher RF drive levels (keeping all devices linear) and high optical power levels (same caveat). The RF match of the modulator and photodiode will also influence uncertainties to some degree (at all signal levels) but the dependence is relatively weak as long as return loss is better than a few dB. For the plots in Figure 15 and Figure 16, a modulator match of -24 dB at low frequencies to -15 dB at 65 GHz and a detector match of -20 dB at low frequencies to -9 dB at 65 GHz were assumed as is typical for some commercial devices. Making both matches worse by 5 dB causes an uncertainty degradation of about 0.15 dB.

On the optical side, there is little high level signal dependence as long as the devices are operating linearly. The characterized photodiodes are usually chosen to be very linear over wide power ranges to keep this from being an issue. The characterized detectors typically also have very weak wavelength dependencies; usually less than a few hundredths of a dB over 40 nm. When using a modulator as a transfer standard (as in an O/E measurement), however, it is important that the same wavelength be used in the different measurements with that modulator since much greater wavelength sensitivity usually exists in that component (although this will vary with technology). Specifications for the Anritsu MS4647X VNA and 3654D V Calibration Kit were used to calculate VNA uncertainties at various frequencies. The use of different VNAs and/or calibration kits may result in slightly different values. Characterization uncertainties of the MN4765B O/E calibration device were used for the standard part of the model. Optical system drift is included in the error model but it is assumed that all components are mechanically and thermally stable. Connector repeatability is also included in the model but all connectors are assumed to be in very good condition. The results are shown with an independent variable of photodiode output power and plotted for both magnitude and phase for the two different types of measurements. Frequency is used as a parameter. While the results for a two port measurement are shown here, there are normally no significant deviations in going to four port structures.

<sup>6</sup> D. F. Williams, P. D. Hale, T. S. Clement, and J. M. Morgan, "Calibrating electro-optic sampling systems," 2001 Int. Micr. Symp. Dig., pp. 1527-1530, May 2001.

<sup>7</sup> P. D. Hale and C. M. Wang, "Calibration service for evaluating and expressing optoelectronic frequency response at 1319nm for combined photodiode/RF power sensor transfer standards," NIST Special Publ. 250-51, 1999.

<sup>8</sup> -, "What is your measurement accuracy," Anritsu application note 11310-00270, 2001.

As can be seen in Figure 15 and Figure 16, the uncertainty reaches an asymptote for detector output levels above about  $-60$  dBm. Above this level, the dominant source of uncertainty passes from measurement signal-to-noise ratio to characterization uncertainty.

There is some frequency dependence for several reasons:

1. Noise floor is higher at higher frequencies.
2. The characterization uncertainty goes up with frequency.
3. The basic VNA uncertainty (due to residual mismatch, etc.) goes up with frequency.

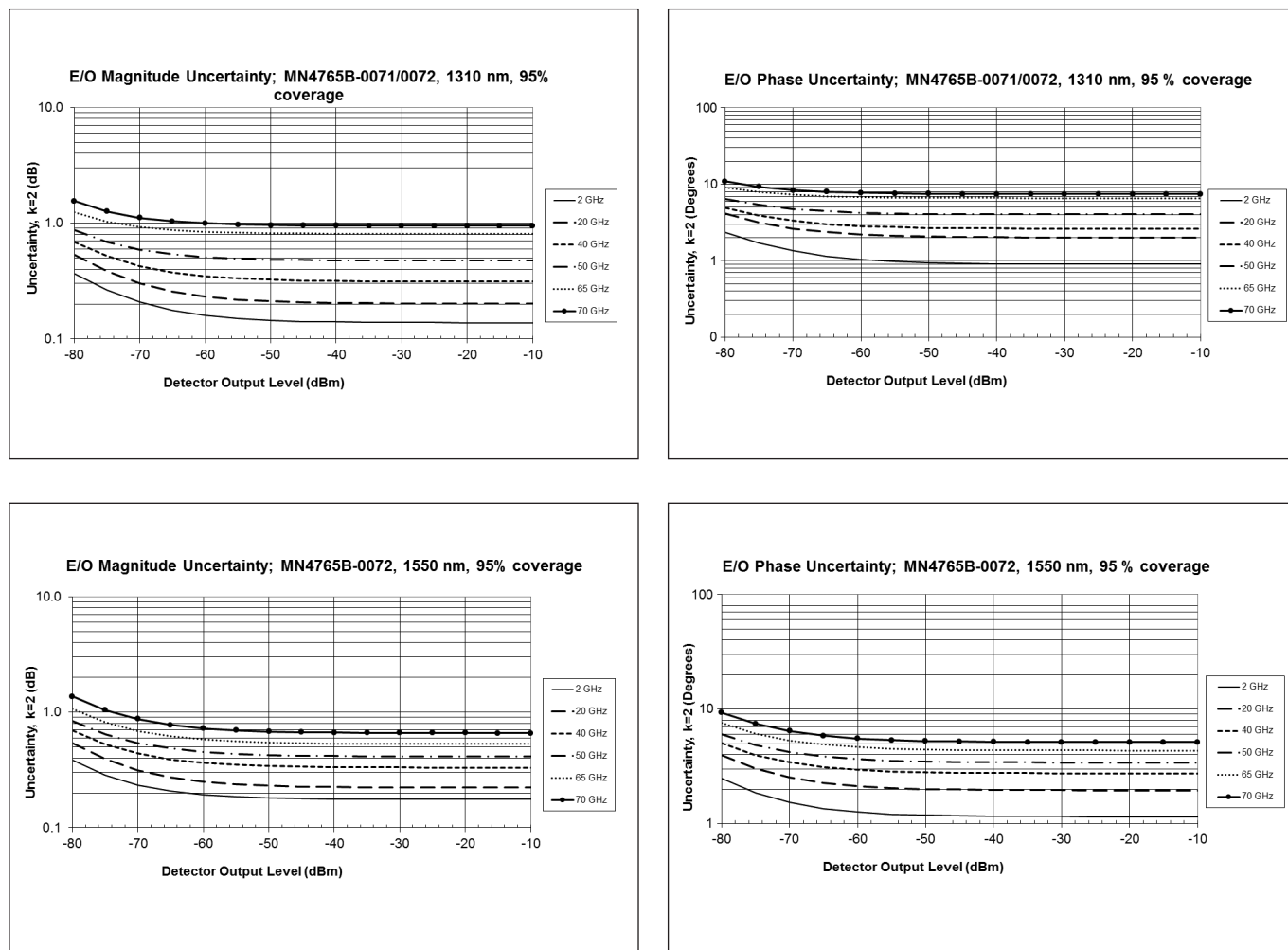


Figure 15: Example E/O measurement uncertainty plots are shown here for the conditions discussed in the text.

A few additional caveats are necessary on these curves:

- Older MN4765A's were characterized on a different VNA platform (37XXX) that had different base uncertainties particularly in terms of the noise floor at higher frequencies. The characterization data for those modules has that uncertainty built in and, hence, the optical converter measurements, even if performed on a MS464XX VNA will be somewhat elevated (by about 0.5 dB in E/O magnitude at -50 dBm and 65 GHz; less at lower frequencies and higher power levels). Uncertainties for 37XXX-based characterization and measurement are published in an older application note . The uncertainties for a MS464XX-measured but 37XXX-characterized setup will be part way between the curves published in that older application note and the curves published here.
- The 70 GHz characterization may not be available on all MN4765As as that data has not propagated through to all devices. If the characterization file only reaches 65 GHz, no uncertainty is defined above that frequency.
- All MN4765B models are MS464XX-characterized from 70 kHz to 40/70/110 GHz (depending on the module option).
- The MN4765B-0072 is characterized at both 1310 and 1550 nm wavelengths and this is reflected in the curves. The difference between uncertainties at the two wavelengths is small.

The MN4765B-0040 is characterized at 850 and 1060 nm. The MN4765B-0043 is characterized at all four wavelengths (850/1060/1310/1550 nm).

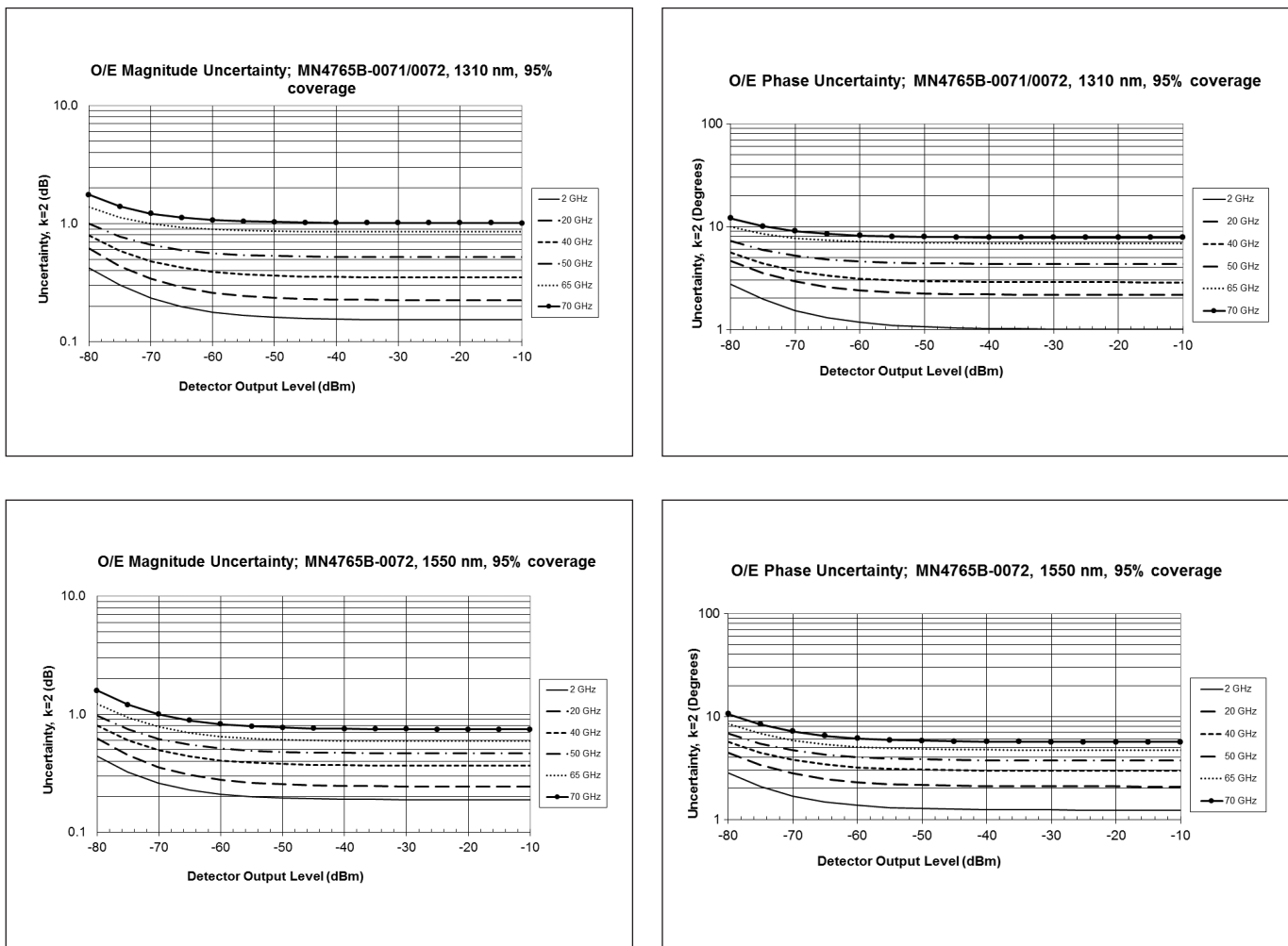


Figure 16: Example O/E measurement uncertainty plots are shown here for the conditions discussed in the text.

Since we have not been exhaustive in including all uncertainty curves (this is an app note so the hope was just to convey the general shapes of curves and what parameters are relevant), we probably will not add 850nm curves here.

## Summary

The E/O and O/E measurement utilities have been discussed in this application note. This utility is essentially an advanced de-embedding tool allowing one to remove the effects of one optical conversion device to learn the properties of the other. There are a large number of configuration choices, particularly in the four port cases, but the measurement principle is the same: use a good VNA calibration to characterize the converting pair and then de-embed the effects of a calibrated/characterized device to analyze the DUT. Signal-to-noise ratio is often a limiting uncertainty factor so it is important to carefully choose drive levels (as high as possible without being nonlinear), IF bandwidth, and averaging in order to optimize the measurements.

## • United States

### Anritsu Company

1155 East Collins Boulevard, Suite 100,  
Richardson, TX, 75081 U.S.A.  
Toll Free: 1-800-267-4878  
Phone: +1-972-644-1777  
Fax: +1-972-671-1877

## • Canada

### Anritsu Electronics Ltd.

700 Silver Seven Road, Suite 120,  
Kanata, Ontario K2V 1C3, Canada  
Phone: +1-613-591-2003  
Fax: +1-613-591-1006

## • Brazil

### Anritsu Eletrônica Ltda.

Praça Amadeu Amaral, 27 - 1 Andar  
01327-010 - Bela Vista - Sao Paulo - SP - Brazil  
Phone: +55-11-3283-2511  
Fax: +55-11-3288-6940

## • Mexico

### Anritsu Company, S.A. de C.V.

Av. Ejército Nacional No. 579 Piso 9, Col. Granada  
11520 México, D.F., México  
Phone: +52-55-1101-2370  
Fax: +52-55-5254-3147

## • United Kingdom

### Anritsu EMEA Ltd.

200 Capability Green, Luton, Bedfordshire LU1 3LU, U.K.  
Phone: +44-1582-433280  
Fax: +44-1582-731303

## • France

### Anritsu S.A.

12 avenue du Québec, Batiment Iris 1-Silic 612,  
91140 Villebon-sur-Yvette, France  
Phone: +33-1-60-92-15-50  
Fax: +33-1-64-46-10-65

## • Germany

### Anritsu GmbH

Nemetschek Haus, Konrad-Zuse-Platz 1  
81829 München, Germany  
Phone: +49-89-442308-0  
Fax: +49-89-442308-55

## • Italy

### Anritsu S.r.l.

Via Elio Vittorini 129, 00144 Roma Italy  
Phone: +39-06-509-9711  
Fax: +39-06-502-2425

## • Sweden

### Anritsu AB

Kistagången 20B, 164 40 KISTA, Sweden  
Phone: +46-8-534-707-00  
Fax: +46-8-534-707-30

## • Finland

### Anritsu AB

Teknobulevardi 3-5, FI-01530 VANTAA, Finland  
Phone: +358-20-741-8100  
Fax: +358-20-741-8111

## • Denmark

### Anritsu A/S

Kay Fiskers Plads 9, 2300 Copenhagen S, Denmark  
Phone: +45-7211-2200  
Fax: +45-7211-2210

## • Russia

### Anritsu EMEA Ltd.

#### Representation Office in Russia

Tverskaya str. 16/2, bld. 1, 7th floor.  
Moscow, 125009, Russia  
Phone: +7-495-363-1694  
Fax: +7-495-935-8962

## • Spain

### Anritsu EMEA Ltd.

#### Representation Office in Spain

Edificio Cuzco IV, Po. de la Castellana, 141, Pta. 5  
28046, Madrid, Spain  
Phone: +34-915-726-761  
Fax: +34-915-726-621

## • United Arab Emirates

### Anritsu EMEA Ltd.

#### Dubai Liaison Office

P O Box 500413 - Dubai Internet City  
Al Thuraya Building, Tower 1, Suite 701, 7th floor  
Dubai, United Arab Emirates  
Phone: +971-4-3670352  
Fax: +971-4-3688460

## • India

### Anritsu India Pvt Ltd.

2nd & 3rd Floor, #837/1, Binnamangla 1st Stage,  
Indiranagar, 100ft Road, Bangalore - 560038, India  
Phone: +91-80-4058-1300  
Fax: +91-80-4058-1301

## • Singapore

### Anritsu Pte. Ltd.

11 Chang Charn Road, #04-01, Shiro House  
Singapore 159640  
Phone: +65-6282-2400  
Fax: +65-6282-2533

## • P. R. China (Shanghai)

### Anritsu (China) Co., Ltd.

27th Floor, Tower A,  
New Caohejing International Business Center  
No. 391 Gui Ping Road Shanghai, Xu Hui Di District,  
Shanghai 200233, P.R. China  
Phone: +86-21-6237-0898  
Fax: +86-21-6237-0899

## • P. R. China (Hong Kong)

### Anritsu Company Ltd.

Unit 1006-7, 10/F., Greenfield Tower, Concordia Plaza,  
No. 1 Science Museum Road, Tsim Sha Tsui East,  
Kowloon, Hong Kong, P. R. China  
Phone: +852-2301-4980  
Fax: +852-2301-3545

## • Japan

### Anritsu Corporation

8-5, Tamura-cho, Atsugi-shi,  
Kanagawa, 243-0016 Japan  
Phone: +81-46-296-6509  
Fax: +81-46-225-8359

## • Korea

### Anritsu Corporation, Ltd.

5FL, 235 Pangyoyeok-ro, Bundang-gu, Seongnam-si,  
Gyeonggi-do, 13494 Korea  
Phone: +82-31-696-7750  
Fax: +82-31-696-7751

## • Australia

### Anritsu Pty Ltd.

Unit 20, 21-35 Ricketts Road,  
Mount Waverley, Victoria 3149, Australia  
Phone: +61-3-9558-8177  
Fax: +61-3-9558-8255

## • Taiwan

### Anritsu Company Inc.

7F, No. 316, Sec. 1, Neihu Rd., Taipei 114, Taiwan  
Phone: +886-2-8751-1816  
Fax: +886-2-8751-1817

